Seasonal dynamics of autotrophic and heterotrophic plankton metabolism and PCO2 in a subarctic Greenland fjord

Sejr, Mikael K. ; Krause-Jensen, Dorte; Dalsgaard, Tage; Ruiz-Halpern, Sergio ; Duarte, Carlos M.; Middelboe, Mathias; Glud, Ronne N. ; Bendtsen, Jørgen; Balsby, Thorsten J.S.; Rysgaard, Søren

Published in:
Limnology and Oceanography

DOI:
10.4319/lo.2014.59.5.1764

Publication date:
2014

Document version
Publisher's PDF, also known as Version of record

Limnol. Oceanogr., 59(5), 2014, 1764–1778

doi:10.4319/lo.2014.59.5.1764

Seasonal dynamics of autotrophic and heterotrophic plankton metabolism and P_{CO_2} in a subarctic Greenland fjord

Mikael K. Sejr,[1,9,*] Dorte Krause-Jensen,[1,2] Tage Dalsgaard,[1] Sergio Ruiz-Halpern,[3] Carlos M. Duarte,[4,5,6] Mathias Middelboe,[7] Ronne N. Glud,[8,9,10] Jørgen Bendtsen,[9,11] Thorsten J. S. Balsby,[2] and Søren Rysgaard [1,9,12]

[1] Arctic Research Centre, Bioscience, Arhus University, Arhus, Denmark
[2] Department of Marine Ecology, Bioscience, Arhus University, Arhus, Denmark
[3] Centre for Coastal Biogeochemistry, School of Environment, Science and Engineering, Southern Cross University, Lismore, New South Wales, Australia
[4] Department of Global Change Research, Institut Mediterrani d'Estudis Avançats, Consejo Superior de Investigaciones Científicas–Universitat de les Illes Balears, Esporles, Mallorca, Spain
[5] Faculty of Biosciences, Fisheries and Economics, University of Tromsø, Tromsø, Norway
[6] The UWA Oceans Institute and School of Plant Biology, University of Western Australia, University of Western Australia, Crawley, Western Australia
[7] Marine Biological Section, Department of Biology, University of Copenhagen, Copenhagen, Denmark
[8] Southern Danish University and NordCee, Odense, Denmark
[9] Greenland Climate Research Centre, Greenland Institute of Natural Resources, Nuuk, Greenland
[10] Scottish Association of Marine Sciences, Oban, U.K.
[11] ClimateLab, Symbion Science Park, Copenhagen, Denmark
[12] Centre for Earth Observation Science (CEOS), Clayton H. Ridell Faculty of Environmental Earth and Resources, University of Manitoba, Winnipeg, Manitoba, Canada

Abstract

We measured net planktonic community production (NCP), community respiration (CR), and gross primary production (GPP) in September, February, and May in a subarctic Greenland fjord influenced by glacial meltwater and terrestrial runoff. Potential controls of pelagic carbon cycling, including the role of terrestrial carbon, were investigated by relating surface-water partial pressure of CO_2 (P_{CO_2}), NCP, GPP, and CR to physicochemical conditions, chlorophyll a (Chl a) concentration, phytoplankton production, inventories of particulate (POC) and dissolved organic carbon (DOC) and vertical flux of POC. The planktonic community was net heterotrophic in the photic zone in September (NCP = -21 ± 45 mmol O_2 m^{-2} d^{-1}) and February (NCP = -17 mmol O_2 m^{-2} d^{-1}) but net autotrophic during a developing spring bloom in May (NCP = 129 ± 102 mmol O_2 m^{-2} d^{-1}). In September, higher temperatures, shorter day lengths, and lower Chl *a* concentrations compared with May caused increased rates of CR, lower GPP rates, and net heterotrophy in the photic zone. The GPP required to exceed CR and where NCP becomes positive was low (in May: 1.58 ± 0.48 μmol O_2 L^{-1} d^{-1} and September: 3.06 ± 0.82 μmol O_2 L^{-1} d^{-1}) and in the range of open ocean values, indicating that allochtonous carbon did not stimulate CR. The P_{CO_2} in the surface water was below atmospheric levels (September average 25.0 ± 0.71 Pa, February 35.4 ± 0.40 Pa, and May 19.8 ± 1.21 Pa), rendering the ecosystem a sink of atmospheric CO_2. NCP was identified as an important driver of surface P_{CO_2}, with high rates of autotrophy and vertical export of POC reducing surface P_{CO_2} during summer. In winter, net heterotrophy added CO_2 to the water column, but this postive effect on P_{CO_2} was balanced by simultaneous cooling of the water column, which decreased P_{CO_2} because of increased solubility of CO_2. High autochthonous production implies a relatively limited influence of allochthonous carbon on pelagic carbon balance and CO_2 dynamics in the fjord.

The coastal oceans, including estuaries and fjords, comprise the land–ocean boundary zone where organic carbon and nutrients exported from land are processed. Inputs of terrigenous carbon and nutrients often increase rates of production and degradation of organic carbon compared with the open ocean, making the coastal ocean important in global carbon budgets despite only constituting about 7% of the world oceans' area (Chen and Borges 2009; Cai 2011). One effect of the elevated biogeochemical activity of the coastal ocean is the significant contribution to the global air–sea CO_2 exchange. Recent budgets suggest that the global outgassing of CO_2 in estuaries of 0.25 Pg C yr^{-1} is matched by a similar (0.25 Pg C yr^{-1}) uptake on the continental shelves. For comparison, the open oceans are believed to have an uptake of 1.5–2.4 Pg C yr^{-1} (Gruber et al. 2009; Cai 2011), but spatial and temporal variability induces large uncertainties in the estimates of air–sea fluxes of CO_2.

The Arctic coastal oceans are strongly influenced by freshwater, which, in addition to exporting carbon and nutrients, also has strong implications on the stratification and mixing (McClelland et al. 2012) locally and even on a global scale via Meridional Overturning Circulation (Rabe et al. 2011; McClelland et al. 2012). In Greenland fjords, an

* Corresponding author: mse@dmu.dk

important source of freshwater originates from melting glaciers. Meltwater runoff creates strong stratification in the summer and can transport large quantities of inorganic particles and dissolved and particulate carbon into the fjords. A seasonal study from East Greenland estimated that about 50% of the annual vertical flux of particulate organic carbon (POC) to the seafloor was of terrestrial origin (Rysgaard and Sejr 2007) and dissolved organic carbon (DOC) in glacial runoff provides a significant input of labile carbon to the Gulf of Alaska (Hood et al. 2009). Glacial meltwater represents a potential source of terrestrial carbon that could stimulate heterotrophic processes in Greenland fjords. In addition, seasonal ice cover combined with increased turbidity associated with glacial runoff decreases light availability, thereby limiting autotrophy, and together these factors could push the community metabolism toward heterotrophy and potential outgassing of CO_2.

The observed changes in climate have increased the focus on the regulatory effect of temperature on the balance between heterotrophy and autotrophy in the Arctic Ocean. The metabolic balance or the net community production (NCP) of planktonic communities refers to the difference between gross primary production (GPP) and community respiration (CR), where NCP = GPP − CR. Heterotrophic communities (CR > GPP and NCP < 0) act as a source of CO_2, whereas autotrophic communities (GPP > CR and NCP > 0) are sinks of CO_2. Deviation from metabolic balance (CR ≈ GPP) can occur if CR and GPP are temporally and spatially uncoupled (Serret et al. 1999) or if allochtonous inputs of carbon or nutrients stimulate GPP or CR disproportionally (Duarte and Prairie 2005). On the basis of the metabolic theory of ecology (Gillooly et al. 2001; Brown et al. 2004), it has been predicted that both respiration and photosynthesis should increase with increasing temperature, but respiration should do so at a faster rate than photosynthesis, suggesting a shift toward heterotrophy in a warmer future (Brown et al. 2004; Lopez-Urrutia et al. 2006). Empirical relationships between temperature and rates of photosynthesis and respiration are consistent with this prediction (Regaudie-De-Gioux and Duarte 2012). However, several studies of bacterial activity in the Arctic have shown that both availability of resources (carbon and nutrients) and temperature have to be considered to understand the regulation of heterotrophic processes in the Arctic Ocean (Middelboe and Lundsgaard 2003; Kirchman et al. 2009; Kritzberg et al. 2010). At present, scarcity of data on autotrophic but especially heterotrophic processes results in poor spatial and temporal resolution and limits the understanding of the controls on the metabolic balance of Arctic coastal ecosystems. Seasonal studies would be especially useful to resolve a system's overall metabolic status since autotrophic and heterotrophic processes are not necessarily coupled in time.

In this study, we measured pelagic metabolism in September, February, and May in a subarctic fjord in West Greenland. The aim was to provide examples of the seasonal variation in the balance between autotrophy and heterotrophy with emphasis on identifying (1) potential physicochemical and biological controls on community metabolism, including the potential role of allochtonous carbon, and (2) the role of plankton community metabolism in controlling surface-water partial pressure of CO_2 (P_{CO_2}).

Methods

Study site—Sampling was performed during three campaigns (September 2007, February 2008, and May 2008) at a main sampling station in central Kobbefjord (depth 100 m at 64°10.12′ N, 51°33.47′ W). Kobbefjord is a part of the extensive Godthaabsfjord complex in West Greenland (Fig. 1). Several large glaciers connect the Godthaabsfjord to the Greenland ice cap. Kobbefjord is 17 km long and 0.8–2 km wide. Maximum depth is 150 m and maximum tidal range is 4.5 m (Richter et al. 2011). The main freshwater input to the fjord is from a river in the innermost part of the fjord. There are no glaciers that drain directly into Kobbefjord, but glacial meltwater enters in late summer from the Godthaabsfjord. Seasonal sea ice forms in the inner basin of Kobbefjord usually around December and breaks up in early May, whereas the outer part of the fjord is ice free year round.

Oxygen production and consumption—Production and consumption of O_2 was determined by light and dark incubations in 120 mL Winkler bottles to determine NCP and CR. On the basis of NCP and CR, GPP of the water column was calculated as GPP = NCP + CR. A 10 liter polyethylene container was filled with water from each incubation depth (1, 10, 20, 40, and 80 m) using a 5 liter Niskin bottle. The container was gently shaken to homogenize the water before it was siphoned into 24 Winkler bottles through a piece of Tygon tubing, allowing the water to overflow for two volume changes. During this process the water was filtered through a 200 μm filter to remove any metazoan plankton. The volume of the bottles was ca. 120 mL but the actual volume of each was used in the calculations. Eight of these received Winkler reagents I and II (720 μL each) immediately for determination of the initial O_2 concentrations, eight others were placed inside two closed grey polyvinyl chloride tubes for incubation in darkness, and the last eight were placed inside two plexiglass tubes for incubation in light (at 80 m only, dark incubation was performed). The tubes with bottles were deployed at the sampling depth for 24 h (48 and 72 h in February) on a mooring. The incubated bottles received Winkler reagents I and II immediately after being retrieved. The O_2 concentration was analyzed with the photometric Winkler technique (Carpenter 1965) as modified by Labasque et al. (2004). Absorbance was read at 466 nm on a Shimadzu 1240 spectrophotometer, recording four readings for each bottle. Results are presented with propagated standard deviations.

In February and May, in situ measurements of CR at 10 m were compared with experimental treatments of increased temperature (6.5°C above in situ temperature) and DOC (glucose added equivalent to final concentration of 450 μmol C L^{-1}). On each occasion, eight bottles of each treatment ("control," "plus carbon," "increased tempera-

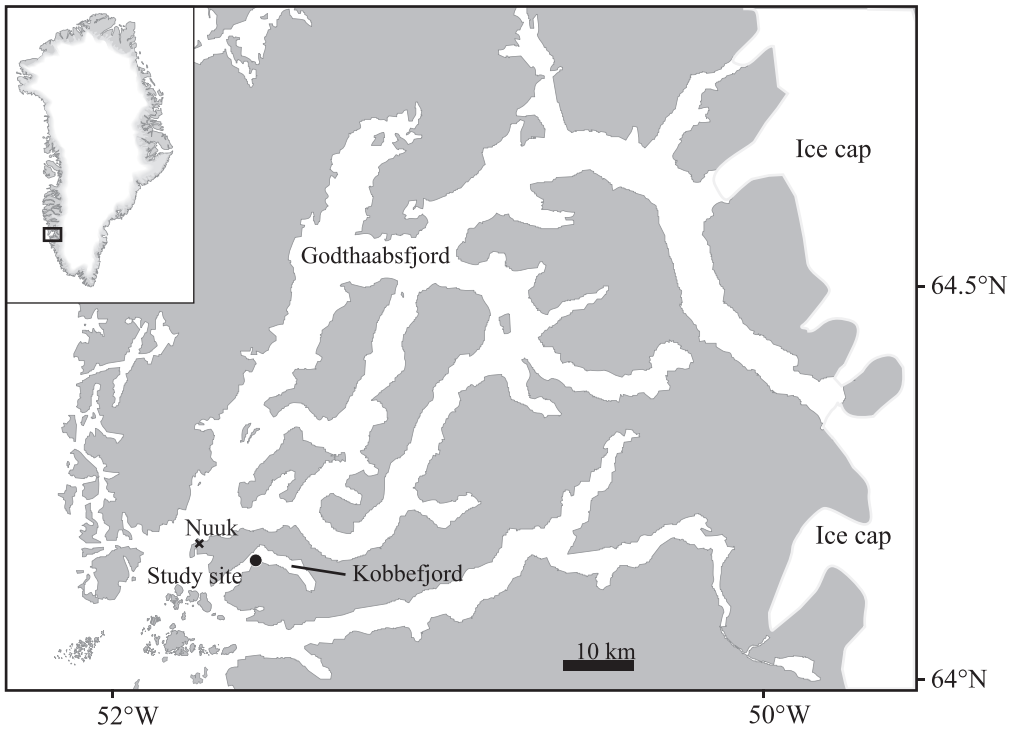

Fig. 1. Map of study area and sampling station.

ture," and "plus carbon and increased temperature combined") were measured. Results were analyzed by subtracting the average start O_2 concentration from the final O_2 concentration in each bottle and testing the effect of treatments using analysis of variance (ANOVA).

Partial pressure of CO_2—The P_{CO_2} was estimated by passing water from a Niskin bottle through Tygon tubing into a membrane equilibrator (Mini Module, Liqui-cel). Air was circulated in a closed system between the equilibrator and an infrared CO_2 analyzer (Environmental Gas Monitor [EGM-4], PP Systems) until a stable reading was obtained (Sejr et al. 2011). These measurements were conducted at different depths at the main station as well as in the surface water along a transect from the river in the inner part of the fjord to the outer part of the fjord.

The role of different carbon sources and sinks for the surface P_{CO_2} was estimated by calculating the relative contribution to the change in surface P_{CO_2} (δP_{CO_2}) between samplings from changes in temperature ($\delta P_{CO_2}[T]$) and the time-integrated contribution from the air–sea flux ($\delta P_{CO_2}[F]$) and NCP (δP_{CO_2}[NCP]): $\delta P_{CO_2} = \delta P_{CO_2}(T) + \delta P_{CO_2}(F) + \delta P_{CO_2}(\text{NCP}) + \delta P_{CO_2}(\text{other})$. The contribution to the change in surface P_{CO_2} from other sources was mainly due to mixing between the surface water with deeper and surrounding water masses but also from the nonlinearity of the surface P_{CO_2} to changes in temperature, salinity, total inorganic carbon (TCO_2), and total alkalinity (TA). The contribution from other sources was not quantified explicitly but was a significant term, in particular during the winter season, as discussed below. The relative change in P_{CO_2} was calculated by estimating TA and TCO_2 by applying the linear relationships to salinity (S) obtained from the surface waters in the nearby Godthaabsfjord (Rysgaard et al. 2012): TA = 161 + 62S (goodness of fit Q = 0.40) and TCO_2 = 169 + 55S (Q = 0.48, where Q is the goodness-of-fit probability; Press et al. 1986). Changes in surface P_{CO_2} between the three periods were then calculated relative to the observed surface temperature and salinity and the corresponding estimated TA and TCO_2 from the equations above. The solubility of CO_2 was calculated according to Weiss (1974) and the air–sea flux was calculated by applying the monthly mean wind speed observed at a local weather station and applying the air–sea exchange parameterization of Wanninkhof (1992). The monthly mean wind speed at the time of the measurements was applied for the whole period between the three observation times because it was found to be relatively constant throughout the year. The annual average wind speed (± SD) was 6.3 ± 0.9 m s^{-1}.

Physicochemical variables, primary production, and vertical flux—At the main sampling station, vertical profiles of temperature, salinity, fluorescence, oxygen, and light intensity (photosynthetically active radioation [PAR], Li-Cor 190SA quantum Q, Li-Cor) were obtained with a conductivity, temperature, depth (CTD) profiler (Sea Bird, SBE19+). Oxygen concentrations are presented as apparent oxygen utilization (AOU), which is the difference between the measured dissolved concentration and its equilibrium saturation concentration in water with the same physical and chemical properties. The photic zone (Z_{eu}) was defined, on the basis of the PAR attenuation (K_d), as extending to 1% of the surface irradiance, i.e., $Z_{eu} = \ln(100/1)/K_d = 4.6/K_d$ (Kirk 1994). A Niskin bottle was used to collect water samples from depths of 1, 10, 20, 40,

and 80 m for analysis of nutrients, chlorophyll *a* (Chl *a*), POC, and DOC. The concentration of $NO_3^- + NO_2^-$ was determined as NO on a NO_x analyzer (Model 42C, Thermo Environmental Instruments) after reduction to NO in hot vanadium chloride (Braham and Hendrix 1989). Phosphate and silicate were determined by standard colorimetric methods and analyzed automatically on a robotic sample processor coupled to a spectrophotometer (Gilson 222 XL and Shimadzu 1600 PC). Detection limits for $NO_3^- + NO_2^-$, phosphate, and silicate were 0.15, 0.20, and 0.25 μmol L^{-1} respectively. Chl *a* was determined by filtration onto GF/C filters (max. 0.3 bar), after which filters were extracted in 96% ethanol for 24 h (at 4°C in the dark) and analyzed fluorometrically (Turner Designs TD-700). Phytoplankton primary production was determined by in situ incubation of 120 mL Winkler glass bottles at 5, 10, 20, 30, and 40 m depth after adding 200 μL of $Na_2{}^{14}CO_3$ with an activity of 20 μCi mL^{-1} (Steemann Nielsen 1952). Two bottles were incubated in the light and one bottle in the dark at each depth for 2 h close to noon. The content of each bottle was filtered onto GF/F filters that were transferred to scintillation vials and 100 μL of 1 mol L^{-1} HCl was added and the filters were fumed for 8 h. After addition of scintillation fluid (UltimaGold+), the samples were measured on a PerkinElmer scintillation counter. On one occasion in May, the total primary production (particulate and dissolved) was measured following the protocol by Moran et al. (2001). Activity in dark bottles was subtracted from light bottles.

Vertical sinking flux of particulate carbon was measured using duplicate free-drifting sediment traps deployed for 2 h at 60 m as described in Sejr et al. (2007). Contents of the traps were filtered onto GF/F filters. Samples for POC content in the water column were also filtered onto precombusted GF/F filters. Filters were frozen and analyzed on an elemental analyzer (Roboprep-CN, Europe Scientific). Water samples for determination of DOC were filtered through precombusted GF/F filters and frozen (−18°C) in combusted 20 mL vials until analysis on a Shimadzu total organic carbon TOC-5000 analyzer.

Statistical analysis—We used a principal component analysis to investigate the effect of the abiotic variables affecting NCP and CR. However, the loadings for both sets of independent variables gave numerically similar loadings for all variables except for chlorophyll and POC (data not shown). This means that the principal component analysis does not enable identification of specific variables that influence the first principal component and therefore does not clarify effects of individual variables. Instead, we first tested the effects of month, day, and depth on NCP and CR using a general linear model followed by tests of the influence that abiotic factors have on CR, GPP, and NCP. Tests were conducted using a general linear model for each month to avoid mixing several different seasonally dependent mechanisms. For February there were too few data to run general linear models. The general linear models only included main factors. For this test CR and NCP were log transformed ($\log[x + 5.2]$) for residuals to be normally distributed.

In the experiment on the effects of temperature and carbon substrate on CR we subtracted the average ($n = 8$) start O_2 concentration from the final O_2 concentration in each of eight bottles and tested the effect of treatments (control, plus carbon, increased temperature, and plus carbon and increased temperature combined) using ANOVA. All statistics were calculated in SAS version 9.2 (SAS Institute).

Results

CTD data—A total of 22 vertical profiles was used to describe the seasonal variation at our sampling station (Fig. 2). In September, the temperature was above 6°C in the top 5 m and most of the water column was above 2°C. Salinity was relatively low in the top 50 m of the water column. Input from the local river is likely visible as a decrease in salinity in the top 5 m of the water column, whereas the decrease down to 50 m is a result of input of water from the larger Godthaabsfjord system, which receives meltwater discharged by several glaciers. Fluorescence was converted to Chl *a* on the basis of the linear regression between measured Chl *a* and fluorescence for the entire September campaign (Chl $a = 1.26 \times$ fluorescence − 0.05, $p < 0.001$, $r^2 = 0.97$). Levels were low, i.e., between 0.5 and 1.5 μg Chl *a* L^{-1}, from the surface down to 40 m.

In February, the water column was fully mixed, with a salinity of 32.8 and a temperature of −1.1°C. The water was undersaturated in oxygen-equivalent AOU values of 15 to 25 μmol O_2 L^{-1}. Fluorescence was low and showed no consistent pattern with depth.

In May, melting of local sea ice and runoff from land had lowered salinity at the surface to around 30, whereas salinity below 10 m had increased slightly to 33.2. Temperature had increased to 0°C below 10 m and up to 4°C at the surface. Fluorescence was converted to Chl *a* equivalents (Chl $a = 1.09 \times$ fluorescence + 0.98, $p < 0.01$, $r^2 = 0.91$). A distinct subsurface peak of 13.8 μg Chl *a* L^{-1} occurred at 10 to 30 m depth and levels of about 2 μg Chl *a* L^{-1} extended all the way to the bottom. This developing spring bloom resulted in supersaturation of the water column, exceeding 80 μmol O_2 L^{-1}, but below 40 m the water was close to saturation and AOU was close to zero.

Nutrients and PAR—In September, $NO_3^- + NO_2^-$ displayed a gradual decrease in concentration from surface to bottom, with low values (0.2 μmol L^{-1}) at 1 m, increasing to 4 μmol L^{-1} at 80 m depth (Fig. 3). Phosphate levels were similar to observations in May, whereas silicate was below detection level from the surface to 40 m depth but with high concentration (3.1 μmol L^{-1}) at 80 m depth. In February, nutrients showed marginal variation with depth and the concentration of $NO_3^- + NO_2^-$ was ~ 9 μmol L^{-1}, phosphate ~ 0.7 μmol L^{-1}, and silicate ~ 1–1.5 μmol L^{-1} throughout the water column. In May, nutrient levels had decreased, especially in the upper 40 m. $NO_3^- + NO_2^-$ was below detection level at 1 and 10 m, increasing to 6 μmol L^{-1} at 40 and 80 m depth. The monthly changes in $NO_3^- + NO_2^-$ observed at 80 m depth are likely related to the inflow of deep coastal water that

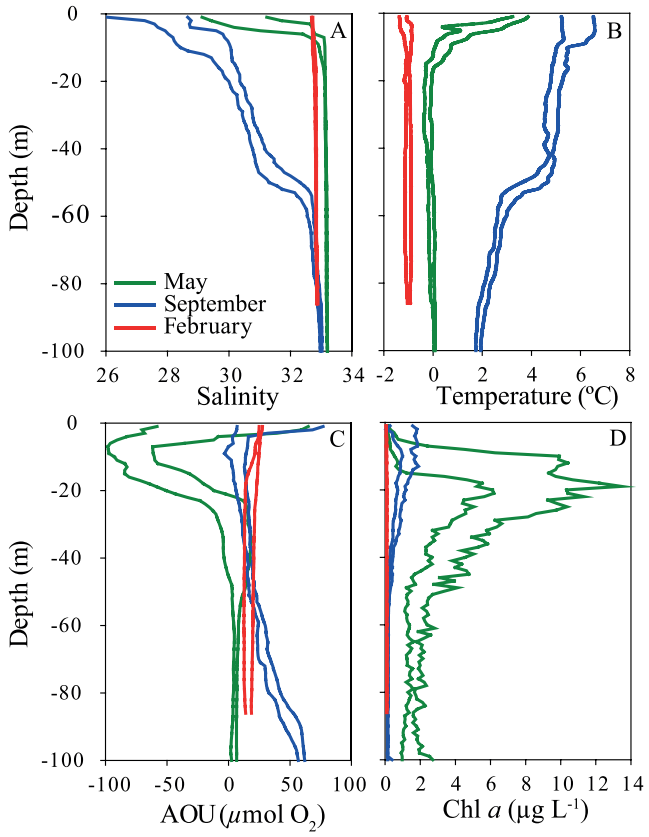

Fig. 2. Range (minimum and maximum values of six to eight daily profiles) observed during the three sampling campaigns in Kobbefjord, West Greenland. (A) Salinity, (B) temperature, (C) apparent oxygen utilization (AOU), and (D) fluorescence-converted Chl *a* values.

regularly takes place in winter and spring (Mortensen et al. 2011). Phosphate concentrations were reduced to about half the winter concentration at 1, 10, and 20 m depth, whereas at 40 and 80 m concentrations were only slightly lower than in February (0.55 μmol L^{-1}). Silicate concentrations were similar to winter values at 1, 40, and 80 m but had decreased to $<$ 0.5 μmol L^{-1} at 10 and 20 m, corresponding to the depths of maximum phytoplankton production.

The PAR attenuation was lowest in February (Table 1) and the photic zone extended down to 56 m. In May, the phytoplankton bloom reduced water clarity and the photic zone only extended down to 21 m. In September, fluorescence had decreased compared with May and the photic zone extended down to 28 m.

Oxygen production and consumption—A considerable challenge when using closed-bottle techniques to estimate plankton production and respiration is to obtain sufficient precision. Across all seasons the average coefficient of variation of each set of eight replicate bottles (initial, light or dark) was 0.28. The oxygen concentration of each set of eight bottles could then (on average) be estimated with a 95% confidence interval of $\pm$ 0.45 μmol O_2 L^{-1}. In practice, this meant that significant differences between the start and end of the incubations as low as 0.6 μmol O_2 L^{-1} were resolved. Estimates of community metabolism from bottle incubations in light and dark are associated with artifacts and limitations, related to confining discrete volumes of water (Duarte et al. 2013). Specifically, bottle effects can artificially increase CR rates. However, studies have documented near-linear changes in O_2 during bottle incubations of 24–48 h (Garcia-Martin et al. 2011) and longer (Nguyen et al. 2012), suggesting that CR rates in this study can be considered a reliable estimate of in situ rates. In the following, all rates related to a decrease in oxygen concentration are reported as negative numbers.

In September, the CR rates were high throughout the water column (Fig. 4). Considerable variation was found between depths and days but without obvious patterns. Respiration rates were generally around -2 to -5 μmol O_2 L^{-1} d^{-1}. GPP showed a consistent pattern, with highest values at 1 m (of around 5 μmol O_2 L^{-1} d^{-1}), decreasing with depth to 0.5 μmol O_2 L^{-1} d^{-1} at 40 m. The relatively high respiration rates confined positive NCP to the upper 10 m.

In February, during the first deployment, bottles were incubated for 48 h and no significant change in oxygen concentration was found in either light or dark bottles

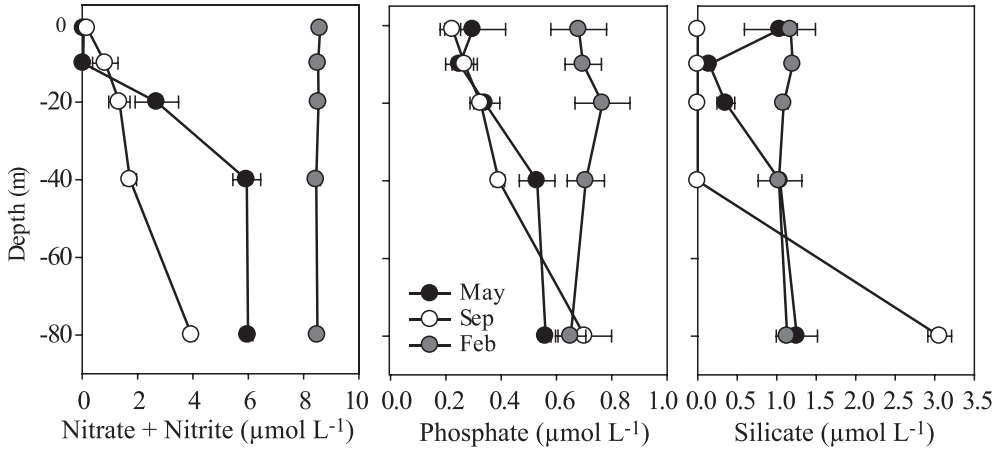

Fig. 3. Seasonal nutrient profiles (average $\pm$ SD) from Kobbefjord, West Greenland.

Table 1. Summary of the duration of average daylight period, light attenuation coefficient, K_d (± SD), and depth of the euphotic zone (Z_{eu}) during the three sampling campaigns in Kobbefjord.

	Daylight (hh:mm)	K_d (m^{-1})	Z_{eu} (m)
Sep	13:07	0.135±0.009	28.3
Feb	9:08	0.083±0.007	55.7
May	19:30	0.197±0.013	20.7

(Fig. 4). The incubation time was therefore increased to 72 h. Still, no significant oxygen production occurred in the light, and rates of GPP were below the detection limit (Fig. 4), but respiration rates of −0.7, −0.3, and −0.4 μmol O_2 L^{-1} d^{-1} were recorded at 10, 20, and 80 m depth. The NCP was consequently negative, with marginal differences between depths and an average oxygen consumption of −0.4 μmol O_2 L^{-1} d^{-1} across depths (Fig. 4).

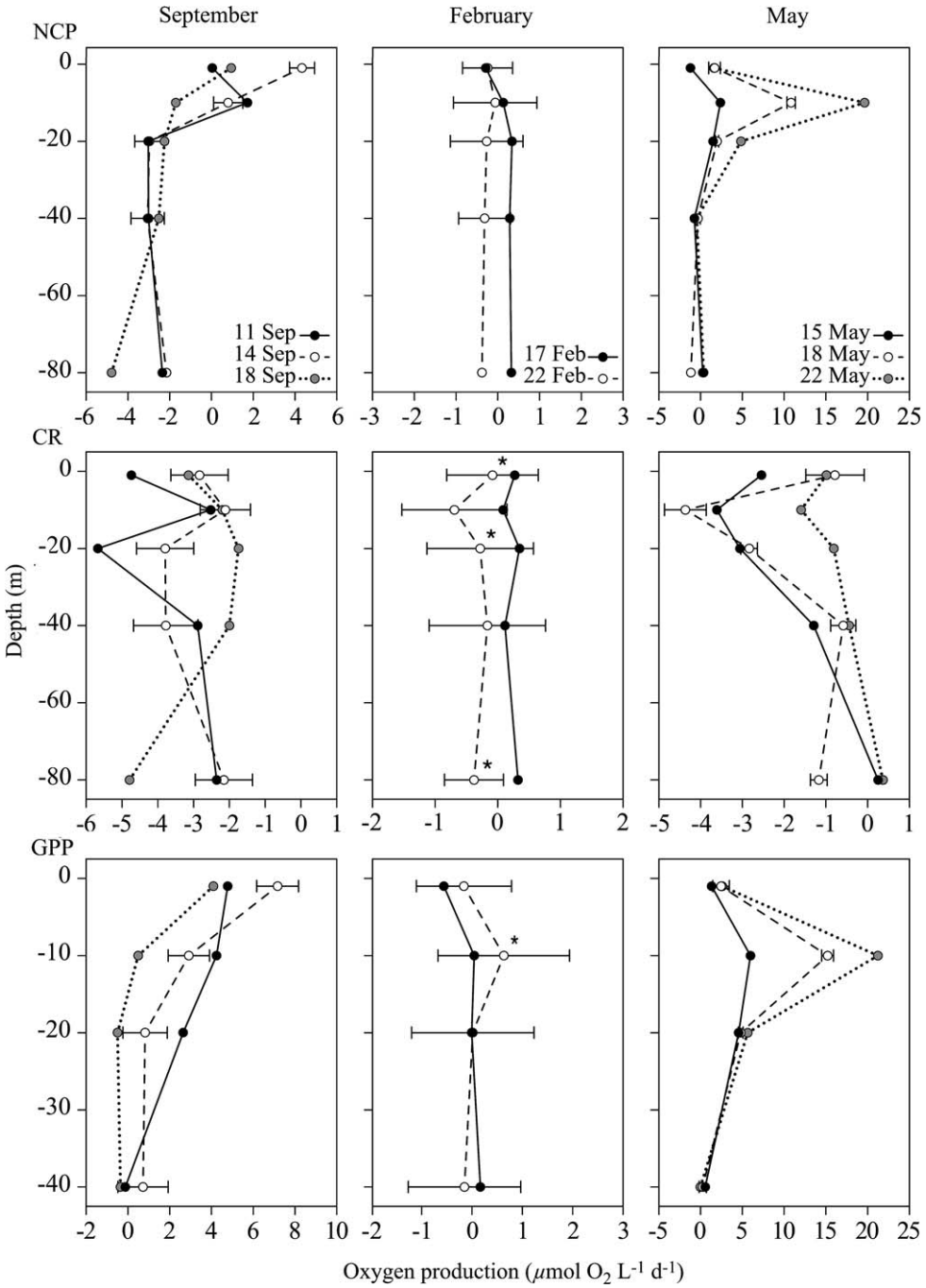

Fig. 4. NCP, CR, and GPP in September, February, and May in Kobbefjord, West Greenland. Error bars (SDs) are only shown for one sampling date per season to avoid clutter. In February, only data points marked with an asterisk showed significant difference between initial and final oxygen concentrations (t-test; $n = 16$, $p < 0.05$).

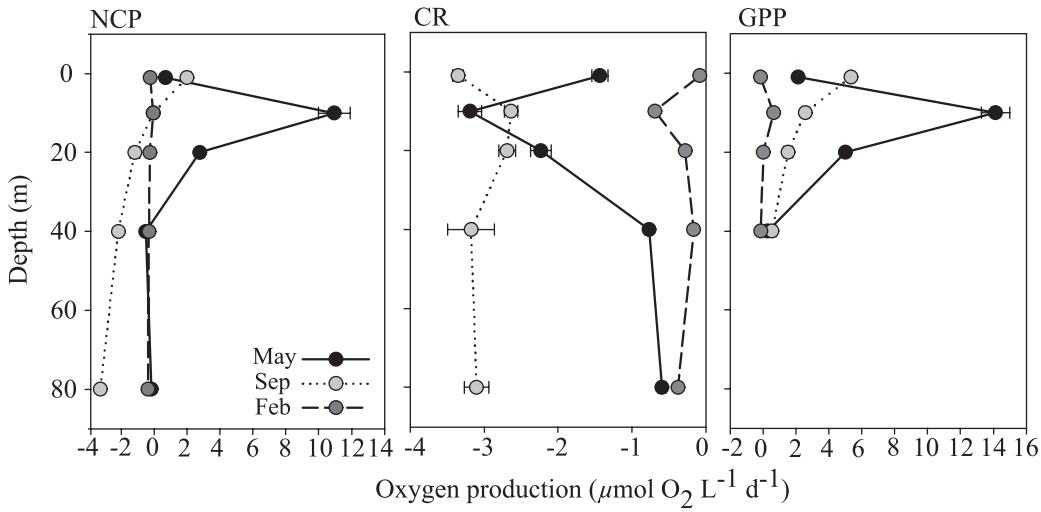

Fig. 5. Seasonal averages (± standard error) of NCP, CR, and GPP in February, May, and September in Kobbefjord, West Greenland.

In May, respiration rates had increased compared with February, with the highest rates found at 10 and 20 m depth. On the third incubation (May 22), respiration rates were lower compared with the two previous incubations (Fig. 4). GPP rates peaked at 10 m depth and showed an increasing trend from about 5 μmol O_2 L^{-1} d^{-1} at the first incubation to more than 20 μmol O_2 L^{-1} d^{-1} on May 22 (Fig. 2). The NCP was positive at 1, 10, and 20 m in May and negative at 40 and 80 m.

In summary, and focusing on average values for each season (Fig. 5), September was characterized by high respiration rates throughout the water column, with rates of -3 to -5 μmol O_2 L^{-1} d^{-1} and GPP limited to the surface waters with rates of around 5 μmol O_2 L^{-1} d^{-1}. In February, low respiration rates and negative NCP values were found throughout the water column. In May high subsurface production (up to 22 μmol O_2 L^{-1}) was found and respiration had increased at 10 m depth compared with February (Fig. 5). A general linear model was used to test the effect of the variables day, depth, and month for CR and NCP. For CR, there was a significant effect of all variables ($R^2 = 0.197$, $F_{8.302} = 9.23$, $p < 0.001$) and depth, month, and day explained 25%, 62%, and 13% of the variation in CR, respectively. For NCP there was also a significant effect of day, month, and depth ($R^2 = 0.455$, $F_{7.229} = 27.36$, $p < 0.001$), which explained 17%, 48%, and 35% of the variation, respectively. A similar test was not conducted for GPP since it is calculated from (average values of) NCP + CR, which removes replicates from the analysis. General linear models were used to identify the effect of specific abiotic drivers on NCP (Table 2) and CR (Table 3). The overall models for the abiotic factors were only significant for NCP in September. In September temperature had a significant effect on NCP. It should be noted that also PAR and P_{CO_2} were close to significance in both May and September. The effect of nutrients (N, P, Si), light (log PAR), and Chl *a* on GPP were analyzed separately for May and September, because between-month variation in GPP would necessitate analyses of interactions with month for all variables. In September Si was omitted from the analysis because only three measurements differed from 0. The overall model with all variables was significant for September (general linear model $F_{5,6} = 6.16$, $p = 0.02$). GPP was positively related to light intensity (log PAR; general linear model estimate = 4.27, $F_{5,6} = 14.73$, $p = 0.009$). The other variables did not vary significantly with GPP (general linear model $F_{1,6} = 2.34$, $p = 0.177$). In May the effect of the variables on GPP was

Table 2. Results of general linear models testing the influence of abiotic factors on NCP for each month separately. Too few data prevented analysis for February.

	May			September		
Log-transformed NCP	df	*F*	*p*	df	*F*	*p*
Overall model	7,4	5.32	0.06	6,5	5.94	0.03
PAR	1,4	4.82	0.09	1,5	5.81	0.06
Nitrate+nitrite	1,4	0.14	0.73	1,5	4.36	0.09
Phosphate	1,4	2.59	0.18	1,5	0.11	0.76
Silicate	1,4	1.37	0.31	na*	na	na
P_{CO_2}	1,4	4.95	0.09	1,5	6.39	0.05
Temperature	1,4	0.09	0.80	1,5	9.79	0.03
Chl *a*	1,4	0.45	0.54	1,5	0.29	0.61

* na, not applicable.

Table 3. Results of general linear models testing the influence of abiotic factors on CR for each month separately. Too few data prevented analysis for February.

	May			September		
Log-transformed CR	df	*F*	*p*	df	*F*	*p*
Overall model	6,8	1.59	0.27	6,8	0.26	0.94
DOC	1,8	0.13	0.73	1,8	0.22	0.65
Nitrate+nitrite	1,8	0.89	0.37	1,8	0.01	0.93
Phosphate	1,8	0.08	0.78	1,8	0.53	0.49
POC	1,8	0.68	0.43	1,8	0.87	0.38
Silicate	1,8	0.01	0.93	1,8	0.68	0.43
Temperature	1,8	0.28	0.61	1,8	0.92	0.37

Table 4. Integrated values (±SD where available) for NCP, CR, and GPP for the photic zone and the entire water column at the sampling station studied in Kobbefjord, West Greenland.

	Integrated values, euphotic zone (mmol O_2 m^{-2} d^{-1})			Integrated values, water column (0–100 m; mmol O_2 m^{-2} d^{-1})		
	NCP	CR	GPP	NCP	CR	GPP
September	−21±45	−120±48	99±112	−189±51	−288±29	99±112
February	−17	−18	1	−31	−32	1
May	129±102	−52±23	182±82	62±42	−120±51	182±82

not detectable, since the overall model was not significant (general linear model $R^2 = 0.598$ $F_{5,6} = 1.24$, $p = 0.41$).

The depth-integrated NCP was negative for the photic zone in September and February but positive in May (Table 4). Linear regression (type II) of NCP against GPP revealed significant linear relationships in May and September (Fig. 6) and the GPP needed to balance respiration increased from 1.58 ± 0.48 μmol O_2 L^{-1} d^{-1} in May to 3.06 ± 0.82 μmol O_2 L^{-1} d^{-1} in September.

The effect of increased temperature and addition of DOC on CR was experimentally tested in February and May. In February, the CR at in situ conditions (at 10 m depth) was −0.7 μmol O_2 L^{-1} d^{-1}. Neither addition of carbon nor increasing temperatures by 6.5°C caused a significant increase in CR (ANOVA $p = 0.31$ and $p = 0.18$ for the effect of carbon and warming, respectively), but carbon addition and warming combined resulted in significantly increased CR (−4.2 μmol O_2 L^{-1} d^{-1}, $p < 0.05$). In May, a similar experiment was conducted and again only when carbon addition was combined with temperatures of 6.5°C above in situ conditions did CR change significantly from −1.6 μmol O_2 L^{-1} d^{-1} in the control to −9.2 μmol O_2 L^{-1} d^{-1} (ANOVA $p < 0.01$).

Partial pressure of CO_2—The P_{CO_2} in the surface water was below atmospheric saturation (approximately 40 Pa) on all sampling occasions (Fig. 7A). At our main sampling site approximately 8 km from the river input to the fjord,

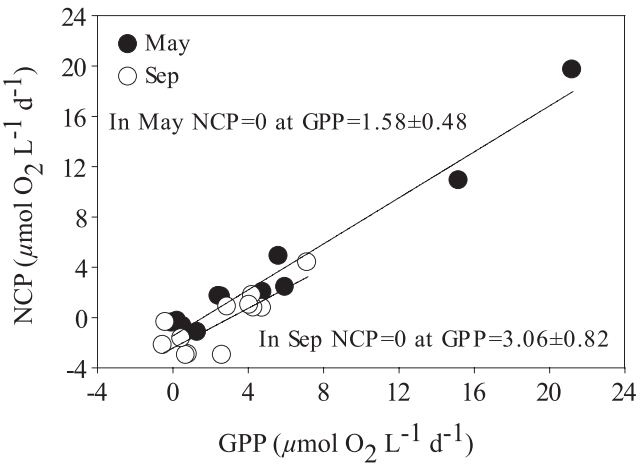

Fig. 6. Linear regressions (± SE) of GPP and NCP in May and September. (May: NCP = 0.91 ± 0.06 × GPP −1.45 ± 0.48. $r^2 = 0.96$, $p < 0.001$; September: NCP = 0.79 ± 0.17 × GPP − 2.41 ± 0.60. $r^2 = 0.67$, $p < 0.01$).

the average (± SD) P_{CO_2} content was 25.0 ± 0.71 Pa in September, 35.4 ± 0.40 Pa in February, and 19.8 ± 1.21 Pa in May. In September and May, additional measurements from the inner to the outer part of the fjord showed that P_{CO_2} increased with distance from the river. This increase was most pronounced in May. Depth profiles of P_{CO_2} (Fig. 7B) also documented P_{CO_2} below atmospheric levels at all water depths. In September, highest P_{CO_2} values were found at 80 m, with a uniform decrease to 25 Pa at the surface. In February, P_{CO_2} was uniform throughout the water column, with values of 36 Pa. In May, the P_{CO_2} at 80 m had decreased to ~30 Pa and the vertical profiles showed a steep decrease from 30 m depth to the surface. The average physicochemical conditions are listed in Table 5 together with the observed change in surface P_{CO_2} between months. Additionally, we calculated contribution to changes in P_{CO_2} between sampling campaigns from three processes: (1) change in temperature, (2) ecosystem metabolism, and (3) air–sea exchange of CO_2. The relative importance of the three processes changed between sampling periods but with NCP generally contributing most. From February to May a considerable remainder of −18.9 Pa could not be explained on the basis of the three processes.

Vertical flux, organic carbon, and ^{14}C primary production—Vertical flux of carbon averaged 296, 16, and 417 mg m^{-2} d^{-1} in September, February, and May, respectively (Table 6). Concentration of POC in September was highest at the surface (ca. 0.2 mg L^{-1}). In February, POC levels were low at 0.1 mg L^{-1} throughout the water column (Fig. 8). In May, POC levels were high, particularly in the top 40 m, coinciding with the phytoplankton bloom. Concentrations of DOC showed a different seasonal pattern from POC. Highest concentration was found in February of about 140 μmol L^{-1}. In May, DOC concentration was about 90 μmol L^{-1} except for a peak at 10 m (125 μmol L^{-1}) coinciding with the maximum phytoplankton production. In September, DOC was around 70 to 80 μmol L^{-1}. Integrated phytoplankton production was very low in February (15 mg C m^{-2} d^{-1}) and increased in May to an average of 635 mg C m^{-2} d^{-1} (Table 6). In September, production was estimated twice, with very different results (181 and 628 mg C m^{-2} d^{-1}), which could be partly related to cloudy conditions one day and clear sky the other. On one occasion (May 23) not only the particulate fraction of the ^{14}C incorporated was measured but also the fraction present in DOC. The total production of both POC and DOC amounted to 1496 mg C

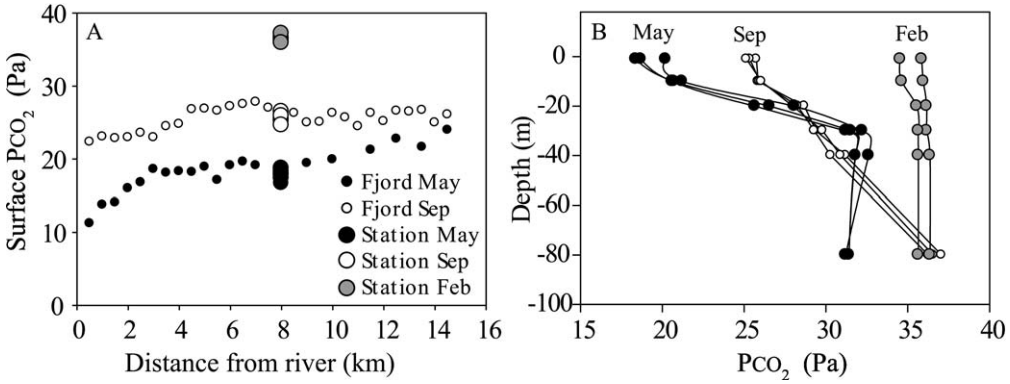

Fig. 7. (A) Seasonal and spatial variation in P_{CO_2} in the surface water of Kobbefjord, West Greenland. Large symbols represents ~ daily measurement during the sampling period. Small symbols show the spatial variation in Kobbefjord investigated in May and September. (B) Profiles of P_{CO_2} at our sampling station.

m^{-2} d^{-1} compared with a POC production of 830 mg C m^{-2} d^{-1} (Table 6). So GPP estimated on the basis of the traditional ^{14}C incubations (GPP-^{14}C) may have underestimated GPP. The depth-specific GPP-^{14}C rates showed a vertical variation very close to that of GPP estimated from O_2 (GPP-O_2), with subsurface peak in May and highest production in September near the surface (data not shown). However, rates of GPP-O_2 were higher than those of GPP-^{14}C. Assuming a photosynthetic quotient of 1.4 (Laws 1991), the average ratio between the O_2- and the ^{14}C-based estimates (mol : mol) was 1.9. This discrepancy can partly be explained by the release of DOC and by the subtraction of activity in dark bottles, which may underestimate production (Legendre 1983). In our data set, ^{14}C counts for samples incubated in the dark were generally less than 10% of those incubated in the light during May and September in the upper 30 m. This percentage rose to 75%, on average, in February. However, the discrepancy between O_2 and ^{14}C data is primarily found when production is high in May and September and omitting the subtraction of dark bottles does not markedly change the ratio between O_2 and ^{14}C measurements. The difference in time span of the GPP-O_2 and GPP-^{14}C incubations also implies that they are not directly comparable.

Table 5. Observed seasonal changes in physicochemical variables at the sampling station in Kobbefjord and the estimated contribution of (1) change in temperature, (2) NCP, and (3) air–sea exchange of CO_2 to the observed changes (between months) in surface P_{CO_2}. *See* Methods for description of how contributions were calculated.

	September	February	May
Observed values			
SST* (°C)	5.66±0.31	−1.18±0.10	3.59±0.22
Salinity	27.9±0.91	32.71±0.02	30.15±0.86
P_{CO_2} (Pa)	25.0±0.71	35.4±0.40	19.8±1.21
Wind speed (m s^{-1})	6.78±2.51	6.85±2.82	5.39±1.91
Mixed layer (m)	22.3±4.8	100	2.8±2.9
Estimated values			
TA (μmol kg^{-1})	1862.9±23.2	2156.3±9.4	2000.2±26.4
TCO_2 (μmol kg^{-1})	1717.5±19.4	2053.5±11.2	1808.5±28.1
	Sep–Feb (ΔPa)	Feb–May (ΔPa)	May–Sep (ΔPa)
Change in P_{CO_2} due to			
Temperature	−7.5	9.7	2.2
NCP	8.2	−14.5	−17.2
Air–sea exchange	7.7	8.1	15.6
Total Pa	8.4	3.3	0.6
Observed change (Pa)	10.4	−15.6	5.2
Remainder (Pa)	2.0	−18.9	4.6

* SST, sea surface temperature.

Discussion

Balance between oxygen production and consumption—The difference between gross production and consumption of oxygen, NCP, varied significantly as a function of depth, day (within month), and between months. Most of the variation was explained by the difference between months related to the change from heterotrophy in September and February to marked autotrophy in the photic zone in May (Fig. 5). Although data do not resolve the full seasonal variation, results are in line with other reports of spring-to-summer transition from autotrophy to heterotrophy (Pomeroy and Wiebe 1993; Serret et al. 1999; Gist et al. 2009). The difference between heterotrophy in September and autotrophy in May was a result of changes in both

Table 6. Integrated values of ^{14}C-estimated particulate primary production. On 23 May the particulate and dissolved primary production was estimated (shown in parentheses). Vertical flux of POC at 50 m depth.

	Primary production (mg C m^{-2} d^{-1})	Vertical flux (mg C m^{-2} d^{-1})	Vertical flux in % of POC production
14 Sep	181	288	159
18 Sep	628	304	48
16 May	425	411	97
19 May	649	529	82
23 May	830 (666)	474	57
19 Feb	16	19	119
23 Feb	13	13	100

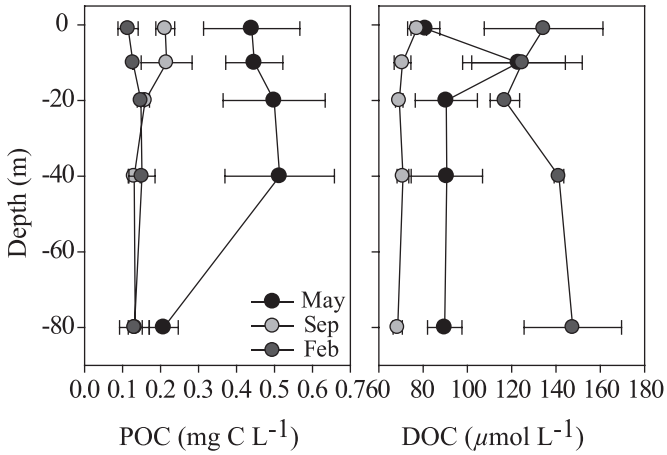

Fig. 8. Vertical distribution of POC and DOC in Kobbefjord, West Greenland.

GPP and CR resulting in the threshold where GPP balances CR to be 1.6 μmol O_2 L^{-1} d^{-1} in May and 3.1 in September (Fig. 6). These values are in range with a general threshold of GPP of the open oceans of 1–3 μmol O_2 L^{-1} d^{-1} found in a meta-analysis (Duarte and Regaudie-De-Gioux 2009), but lower than the 6.4 μmol O_2 L^{-1} d^{-1} found during summer in the Greenland Sea (Regaudie-De-Gioux and Duarte 2010). The average annual threshold of GPP for the European coasts is estimated at 5.0 μmol O_2 L^{-1} d^{-1} (Duarte and Regaudie-De-Gioux 2009). Another study showed that the GPP threshold of planktonic communities is temperature dependent, with predicted threshold values from 1 μmol O_2 L^{-1} d^{-1} in cold water environments to 4 μmol O_2 L^{-1} d^{-1} at 15°C (Lopez-Urrutia et al. 2006). We observed a comparable shift in the GPP threshold from May to September but with an increase in temperature of only ~5°C, indicating that temperature alone was not sufficient to drive the observed change from May to September. That our thresholds are close to the average from the Atlantic Ocean and lower than the average from the European coast suggests that allochtonous carbon from land is not an important driver of the balance between autotrophy and heterotrophy at this coastal site, as significant input of labile carbon from land would be expected to stimulate CR and consequently increase the GPP threshold where GPP = CR. This is supported by a parallel study in Kobbefjord focusing on bacterial carbon consumption (Middelboe et al. 2012). Here, the concentration of bioavailable DOC in the main river was found to be low (144 and 163 μg C L^{-1} in May and September) compared with values in the fjord (ranging between ~200 and 350 μg C L^{-1}) and carbon originating from phytoplankton production was identified as the primary carbon source for the bacterioplankton. In Alaskan streams influenced by glacial meltwater, DOC concentrations ranged from 500 to 1000 μg C L^{-1}, of which 40–60% was bioavailable (Hood et al. 2009). So despite the discharge from a local river to the fjord and discharge of ice and meltwater from six active glaciers into the Godthaabsfjord system, input of labile carbon with this freshwater is apparently low compared with the production in the fjord. The low terrestrial input of labile material in combination with low temperature results in CR values comparable with those in open ocean communities (Regaudie-de-Gioux and Duarte 2010).

The measurements conducted in February are among the few available estimates of the metabolic balance during winter in ice-covered waters. Although measurements were conducted for up to 72 h and rates were close to the detection limit, data show that the turnover of carbon in winter is low but ongoing. Monthly sampling in Kobbefjord in 2007 and 2008 showed low Chl *a* concentration from October through April (Blicher et al. 2010). Short day lengths combined with low temperatures and lack of Chl *a* in the water column suggest that the February measurements could be representative for up to 5 months of the year. Therefore, despite low volumetric rates measured in February, they could influence the annual budget integrated through the winter period. Assuming that February rates are representative for 5 months or 150 d, the winter heterotrophy would consume the NCP of 20 d of spring autotrophy in the photic zone.

In May, the combination of day lengths exceeding 19 h and melting sea ice, which increases the penetration of light to the water column, initiated a pronounced phytoplankton bloom with high autotrophic production. Volumetric rates of NCP of more than 20 μmol O_2 L^{-1} d^{-1} are similar to maximum rates measured in the Fram Strait (Regaudie-De-Gioux and Duarte 2010). The high rates of NCP were reflected in the oxygen profiles in the water column, which showed oversaturation (resulting in negative AOU values) of oxygen of up to 100 μmol O_2 (Fig. 2C), and NCP was positive even when integrating over the entire water column (Table 4). In contrast, NCP was slightly negative in September when integrated over the photic zone, with positive volumetric rates at 1 and on some days also at 10 m depth. However, on a sunny day (September 22) ^{14}C primary production rates matched values from May, indicating that high production can also occur in late summer. Overall, the photic zone in September was in near-metabolic balance, as indicated by AOU values close to zero (Fig. 2). Phytoplankton blooms occur throughout the summer in the central Godthaabsfjord (Jensen 2011), where tidal currents (generated by 4.5 m of tide) entrain nutrients into the photic zone. Daily production as high as 1500 mg POC m^{-2} d^{-1} has been measured in July and the annual production amounts to 76–106 g POC m^{-2} yr^{-1} (Jensen 2011). The Godthaabsfjord system is thus very productive and our single measurement in May where the dissolved fraction of produced organic carbon was included indicates that the total production (particulate and dissolved) of phytoplankton in the fjord could be significantly higher than assessed from the particulate fraction alone. The large potential production of DOC by phytoplankton is also important when interpreting the vertical flux of POC. In our study, as well as in results from the Godthaabsfjord (Jensen 2011), the vertical flux of POC often matches or even exceeds the production of POC estimated from ^{14}C incorporation. On average, we observed that the vertical flux of POC amounted to 95% of the estimated particulate

production, which is in line with other observations in Greenland (Sejr et al. 2007) and also with the observation of high carbon demand by the dominant benthic species in Kobbefjord (Blicher et al. 2009). A 95% loss rate due to vertical flux combined with an estimated bacterioplankton carbon demand in Kobbefjord of 80% of the ^{14}C-derived POC production (Middelboe et al. 2012) suggest that such short-term fluxes are often not closely coupled. The fraction of dissolved to total production averages 45% in our limited measurements (one station, four depths in May) and could contribute substrate to the bacterioplankton. The dissolved fraction can originate from passive diffusion through the cell membrane but may also represent an adaptive process to cope with high light and low nutrient conditions. Our observations in May are high but in the range of other observations in the Arctic (Gosselin 1997).

The variation between monthly average values for NCP integrated for the photic zone in Kobbefjord (range −21 to 129 mmol O_2 m^{-2} d^{-1}) was smaller than the spatial variation in the Chukchi Sea (range −590 to 906 mmol O_2 m^{-2} d^{-1}; Cottrell et al. 2006) and the Greenland Sea (range −303 to 389 mmol O_2 m^{-2} d^{-1}; Regaudie-De-Gioux and Duarte 2010). Day-to-day variation within months was significant in our study, explaining 17% of the total variation for NCP. Especially in May, the progressive increase in NCP at 20 m depth contributed to within-month variation.

Short-term variability (days) is seldom quantified in ship-based studies, which generally consider spatial heterogeneity or coarse seasonality (e.g., monthly sampling frequency). This study showed that for NCP and GPP the total range in values within a week in May exceeded the difference between average values for May and September. The developing bloom, which resulted in increasing Chl *a* concentrations of 1.8, 4.1, and 7.3 μg L^{-1} at 10 m during sampling in May, clearly explains much of the variation. Although much of the daily variation in NCP could be attributed to a spring bloom, which is a well-known seasonal phenomenon in the Arctic, data for both CR and NCP show that daily variation within months constituted 13% (CR) and 17% (NCP) of the total variation (day, month, and depth), which underlines the need to consider daily variation in studies of spatial and seasonal variation. Cloud cover and tidal and wind mixing in a fjord with a tidal amplitude of 4.5 m are likely sources of day-to-day variation. It is clear that the current data set is insufficient to fully resolve the annual variation of autotrophic and heterotrophic processes and constrain carbon stocks, but we find that the data provide instructive examples of seasonal conditions in the area.

Partial pressure of CO_2—Surface P_{CO_2} was below atmospheric saturation at the main station on all sampling occasions and reflected the spatial variation in Kobbefjord in May and September (Fig. 7). Our measurements in Kobbefjord in May, February, and September indicate that the fjord acts as a sink for atmospheric CO_2, which, combined with other available data (Nakaoka et al. 2006; Sejr et al. 2011; Rysgaard et al. 2012), suggests that the coastal and shelf regions of Greenland are an important sink for atmospheric CO_2. A precise quantification of the processes that drive the seasonal changes in surface P_{CO_2} and the observed uptake of CO_2 is not possible from the current data set. However, on the basis of linear interpolation of physicochemical data between sampling periods, a first attempt is presented in Table 5. Of the three variables, whose influence on the seasonal variation in P_{CO_2} we have attempted to quantify (Table 5), NCP appears to be the primary driver responsible for keeping the surface P_{CO_2} below atmospheric saturation. It seems likely that the atmospheric uptake of CO_2 in Kobbefjord is driven by the biological pump by which much of the organic carbon produced in the photic zone is transported below the mixed layer. The autotrophic dominance in the photic zone in spring and potentially throughout the summer combined with stratification due to freshwater from land and high vertical flux of POC ensures a separation of production and mineralization of organic carbon. However, it is clear that the effect of temperature, NCP, and air–sea exchange alone cannot explain the observed change in P_{CO_2} between months and that other factors are equally important, especially from February to May, where a large amount of variation in P_{CO_2} ("remainder" in Table 5) cannot be attributed to changes in temperature, NCP, or air–sea exchange. An important process, the influence of which we could not quantify, is lateral advection (*see* below).

The lack of supersaturation of CO_2 even at depth suggests that advection either prevents CO_2 from building up in Kobbefjord or transports carbon out before being remineralized. Another explanation of the lack of supersaturation is that periods of heterotrophy coincide with cooling of the surface water, which increases the solubility of CO_2 and hence decreases P_{CO_2}. In our estimate of the September-to-February change in P_{CO_2}, the calculated effect of heterotrophy is matched by the effect of cooling. There are considerable uncertainties related to the estimates presented in Table 5, primarily due to the coarse seasonal and spatial resolution. As discussed below, NCP is highly variable and our measurements in May and September are most likely not representative for conditions during summer. Also, a better estimate of the mixed-layer depth throughout the year is important. Since the atmospheric CO_2 taken up by the air–sea exchange is distributed over the mixed layer, a better quantification of the mixed-layer depth would improve the reliability of the current estimate. Finally, the effect of mixing, either vertically or with surrounding water masses, was not quantified but advection and mixing are certainly important for the surface P_{CO_2}, as vertical gradients exist during most of the year. Inflow of coastal water into the fjords in late winter as described by Mortensen et al. (2011) most likely explains the changes in P_{CO_2} and salinity from February to May at 80 m depth. Winter inflow of different water masses could be the process causing the large unexplained remainder in the Februay-to-May change in surface P_{CO_2} (Table 5). In the central Godthaabsfjord, winter inflow and mixing of subpolar mode water has been linked with occasional observations of supersaturated surface water and outgassing of CO_2 (Rysgaard et al. 2012), indicating that advection and mixing of water masses can shift the

direction of the flux of CO_2 between sea and atmosphere. Variation in both NCP and P_{CO_2} in the Godthaabsfjord system is most likely linked to the degree of vertical mixing, as this directly influences the transport of both nutrients and CO_2 from deep water to the surface.

The very-low P_{CO_2} values in May resulting from high NCP in the spring bloom and freshening of the fjord suggests that CO_2 may be limiting primary production during the late spring and early summer. Enhanced primary production in response to increasing CO_2 concentrations is well documented experimentally (Riebesell et al. 2007; Feng et al. 2009) and Hein and Sand-Jensen (1997) reported widespread increased primary production in response to experimentally enhanced CO_2 across the Atlantic Ocean. Thus, phytoplankton photosynthesis may experience CO_2 limitation in situations where mineral nutrients are abundant and P_{CO_2} in the photic zone is low, as is the case in the Arctic during the spring bloom (Takahashi et al. 2002; Sakshaug et al. 2009). CO_2 limitation of primary production in Greenland coastal waters could possibly lead to a fertilization effect of increased atmospheric concentrations of CO_2 on phytoplankton, as suggested for other areas (Riebesell et al. 2007; Feng et al. 2009).

Factors affecting GPP—In May, GPP and Chl *a* concentrations increased progressively during the three consecutive sampling events, indicating that sampling coincided with the development of the spring bloom. The bloom formed at 10–20 m depth, with highest GPP rates at 10 m depth where light and nutrient conditions were optimal, indicating that the upper vertical boundary of the bloom was limited by low levels of nitrogen and CO_2, whereas the deeper boundary was light limited, a typical situation during Arctic spring blooms (Tremblay et al. 2008). In September, nutrient conditions had changed so that no silicate was detectable in the upper 40 m and NO_3^- + NO_2^- concentrations were at a detectable level. Compared with May, day length was reduced by 6 h in September and both GPP- ($p < 0.05$, $n = 12$, $R^2 = 0.65$) and ^{14}C-estimated primary production ($p < 0.05$, $n = 15$, $R^2 = 0.72$) showed linear correlation to log-transformed PAR values, which indicates light limitation in September, whereas nitrogen limitation seems more important in May.

In the central part of the Godthaabsfjord system, multiple blooms form throughout the summer, with maximum production observed in August (Jensen 2011). Maximum Chl *a* concentration in Kobbefjord of 5 μg L^{-1} at 15 m depth was also found in August (Blicher et al. 2010). The presence of several summer blooms and the resulting high annual production is most likely linked to strong tidal currents combined with fjord sills, which cause mixing of nutrients into the photic zone throughout the summer. The recorded variation over a few days was in the same range as the variation between May and September, suggesting that factors operating on relatively short timescales, like local weather conditions, are important. Similar importance of short-term events such as wind-driven upwelling has been reported (Bonilla-Findji et al. 2010). Just as episodic events can cause temporal variation, the spatial variation in GPP can be significant (Cottrell et al. 2006; Regaudie-De-Gioux and Duarte 2010). In the Godthaabsfjord, measurements of primary production using ^{14}C have revealed large spatial variation primarily related to the degree of vertical stratification influenced by distance to glaciers and bathymetry in the fjord (Arendt et al. 2010). The limited seasonal ice cover in Kobbefjord, compared with more northern sites as Disko Bay (69°N) and Young Sound (74°N), results in a much longer season, with light available for production in the Godthaabsfjord (290 d) compared with Disko Bay (190 d) or Young Sound (85 d; Sejr et al. 2009). Accordingly, the estimated annual phytoplankton production in Young Sound is 10 g C m^{-2} yr^{-1} (Rysgaard et al. 1999), compared with 76–106 g C m^{-2} yr^{-1} in the Godthaabsfjord (Jensen 2011). Variation in duration of seasonal ice cover was also shown as an important factor driving spatial variation in benthic primary production by kelp in Greenland fjords (Krause-Jensen et al. 2012). However, nutrient levels in winter are higher in the Godthaabsfjord than in Young Sound (Jensen 2011), which, together with stronger mixing due to a larger tidal amplitude, makes the subarctic Godthaabsfjord more productive. Assuming that annual GPP is lower in areas with longer sea-ice cover, a shift in the community metabolism toward heterotrophy with even low input of allochthonous carbon from land can be expected.

Factors affecting CR—Considerable seasonal and vertical variation was found in CR, although the variation was lower than for GPP. CR was significantly correlated with temperature (Pearson correlation; $p < 0.01$, $n = 34$, $R^2 = 0.29$) but not to DOC concentration, which was higher in winter (Pearson correlation; $p = 0.24$, $n = 34$, $R^2 = 0.12$). Experiments in February and May both showed that single-factor manipulations (carbon or temperature) could not stimulate a significant increase in CR. Only when addition of carbon was combined with increasing temperature was a significant increase observed. Comparable experiments conducted in the Greenland Sea also concluded that temperature and substrate availability together regulated CR (Kritzberg et al. 2010). The seasonal variation of CR in Kobbefjord also supports this combined regulation of CR as indicated by higher CR rates in September compared with February and May, which coincides with an increase in temperature. Furthermore, the concentration of bioavailable DOC (quantified from oxygen consumption experiments run for 10 d) near the surface was higher in September compared with May (Middelboe et al. 2012). This indicates that the high level of DOC in February was relatively refractory, which agrees with the experiments where amendments of labile DOC were required for an increase in CR with increased temperature. The high DOC concentration in February was, therefore, probably a result of lower bacterial consumption due to low temperature and a more refractory pool of DOC. In addition to the pools of DOC and POC, volatile organic carbon contributed significantly to the organic carbon inventory, averaging approximately 30% of the DOC pool (Ruiz-Halpern et al. 2010). Since volatile carbons are not included in either POC or DOC inventories, they constitute a rarely quantified pool of carbon whose role in pelagic carbon cycling remains to be quantified.

The following conclusions could be made with regard to carbon cycling in this seasonally ice-covered Greenland fjord. (1) Production estimated as GPP on the basis of ^{14}C incorporation was high, with a spring bloom in May but with production throughout the summer and fall. In September, light rather than nutrients appears to be limiting GPP. (2) CR was generally low, resulting in thresholds where GPP = CR is in range with values of the open ocean, indicating that allochtonous carbon from land was not important for ecosystem metabolism, a finding supported by concentrations of labile DOC in the river discharging into in Kobbefjord being lower than the concentration in the fjord (Middelboe et al. 2012). (3) CR in winter was low (average -0.4 μmol L^{-1} d^{-1}), and is one of the few available estimates of winter respiration in Arctic waters. On an annual scale, winter respiration was significant and could represent conditions existing for up to 150 d. (4) P_{CO_2} was below atmospheric saturation in surface water and in vertical profiles on all sample dates, indicating that the fjord was an annual sink for atmospheric carbon. (5) Community metabolism appears to be an important driver of the seasonal variation in surface P_{CO_2}. Autotrophy combined with high vertical transport of particulate carbon out of the photic zone drives uptake of atmospheric carbon in summer. (6) During winter, the influence of heterotrophy on surface P_{CO_2} appears to be equivalent to the opposite effect exerted by cooling, resulting in surface water below atmospheric saturation also in February.

The influence of terrestrial carbon on coastal marine ecosystems depends on the ratio between autochthonous and allochthonous carbon, which varies locally depending on the distance from the meltwater source. In the Godthaabsfjord the input of glacial meltwater has been shown to influence pelagic (Tang 2011) and benthic (Sejr et al. 2010) ecosystem structure. At the site of this study, high autochthonous production limits the relative influence of terrestrial carbon and the primary effect of the freshwater is on the physical structure of the water column. In fjords with more pronounced ice cover the autochtonous production can be expected to be lower and hence terrestrial carbon could exert a stronger control on the metabolic balance. The high Arctic Young Sound in East Greenland is ice covered 8–9 months per year, which limits annual pelagic production to about 10 g C m^{-2} yr^{-1} (Rysgaard et al. 1999) or about 10% of the estimated annual production in the Godthaabsfjord. In Young Sound, it has been estimated that 40% of the annual flux of organic particles to the seafloor is of terrestrial origin, indicating that allochthonous carbon can be an important factor for the coastal ecosystems in Greenland (Rysgaard and Sejr 2007). More studies on the local and regional variability are needed before the effects of a melting ice cap on Greenland coastal water can be assessed.

Acknowledgments

Thomas Juul-Pedersen and Flemming Heinrich from the Greenland Institute of Natural Resources are greatly acknowledged for help during fieldwork. Asiaq kindly provided wind data. Two reviewers are greatly acknowledged for constructive comments that improved the manuscript.

This study was financed by a grant from the Commission for Scientific Research in Greenland (KVUG) and by the European Union's Seventh Framework Programme, grant agreement 226248–Arctic Tipping Points and is a contribution to the Greenland Ecosystem Monitoring program. M.M. was supported by the Danish Council for Independent Research (09-072829) and the Carlsberg foundation. S.R. was supported from the project "Depicting Ecosystem–Climate Feedbacks from Permafrost, Snow and Ice" (DEFROST) of the Nordic Centre of Excellence programme "Interaction between Climate Change and the Cryosphere". We gratefully acknowledge the contributions of Arctic Research Centre (ARC), Aarhus University. Support was also provided by the Canada Excellence Research Chair (CERC). This work is a contribution to the Arctic Science Partnership (ASP) asp-net.org.

References

Arendt, K. E., T. G. Nielsen, S. Rysgaard, and K. Tonnesson. 2010. Differences in plankton community structure along the Godthabsfjord, from the Greenland Ice Sheet to offshore waters. Mar. Ecol. Prog. Ser. **401:** 49–62, doi:10.3354/meps08368

Blicher, M. E., S. Rysgaard, and M. K. Sejr. 2010. Seasonal growth variation in Chlamys islandica (Bivalvia) from sub-Arctic Greenland is linked to food availability and temperature. Mar. Ecol. Prog. Ser. **407:** 71–86, doi:10.3354/meps08536

———, M. K. Sejr, and S. Rysgaard. 2009. High carbon demand of dominant macrozoobenthic species indicates their central role in ecosystem carbon flow in a sub-Arctic fjord. Mar. Ecol. Prog. Ser. **383:** 127–140, doi:10.3354/meps07978

Bonilla-Findji, O., J. P. Gattuso, M. D. Pizay, and M. G. Weinbauer. 2010. Autotrophic and heterotrophic metabolism of microbial planktonic communities in an oligotrophic coastal marine ecosystem: Seasonal dynamics and episodic events. Biogeosciences **7:** 3491–3503, doi:10.5194/bg-7-3491-2010

Braman, R. S., and S. A. Hendrix. 1989. Nanogram nitrite and nitrate determination in environmental and biological materials by vanadium (III) reduction with chemilumimescence. Anal. Chem. **61:** 2715–2718, doi:10.1021/ac00199a007

Brown, J. H., J. F. Gillooly, A. P. Allen, V. M. Savage, and G. B. West. 2004. Toward a metabolic theory of ecology. Ecology **85:** 1771–1789, doi:10.1890/03-9000

Cai, W.-J. 2011. Estuarine and coastal ocean carbon paradox: CO_2 sinks or sites of terrestrial carbon incineration? Annu. Rev. Mar. Sci. **3:** 123–145, doi:10.1146/annurev-marine-120709-142723

Carpenter, J. H. 1965. The Chesapeake Bay Institute technique for the Winkler dissolved oxygen method. Limnol. Oceanogr. **10:** 141–143, doi:10.4319/lo.1965.10.1.0141

Chen, C. T. A., and A. V. Borges. 2009. Reconciling opposing views on carbon cycling in the coastal ocean: Continental shelves as sinks and near-shore ecosystems as sources of atmospheric CO_2. Deep Sea Res. II **56:** 578–590, doi:10.1016/j.dsr2.2009.01.001

Cottrell, M. T., R. R. Malmstrom, V. Hill, A. E. Parker, and D. L. Kirchman. 2006. The metabolic balance between autotrophy and heterotrophy in the western Arctic Ocean. Deep Sea Res. I **53:** 1831–1844, doi:10.1016/j.dsr.2006.08.010

Duarte, C., and Y. Prairie. 2005. Prevalence of heterotrophy and atmospheric CO_2 emissions from aquatic ecosystems. Ecosystems **8:** 862–870, doi:10.1007/s10021-005-0177-4

———, and A. Regaudie-De-Gioux. 2009. Threshold of gross primary production for the metabolic balance of marine planktonic communities. Limnol. Oceanogr. **54:** 1015–1022, doi:10.4319/lo.2009.54.3.1015

———, ———, J. M. Arrieta, A. Delgado-Huertas, and S. Agustí. 2013. The oligotrophic ocean is heterotrophic. Annu. Rev. Mar. Sci. **5:** 551–269, doi:10.1146/annurev-marine-121211-172337

Feng, Y., and others. 2009. Effects of increased P_{CO_2} and temperature on the North Atlantic spring bloom. I. The phytoplankton community and biogeochemical response. Mar. Ecol. Prog. Ser. **388:** 13–25, doi:10.3354/meps08133

Garcia-Martin, E., P. Serret, and M. Perez-Lorenzo. 2011. Testing potential bias in marine plankton respiration rates by dark bottle incubations in the NW Iberian shelf: Incubation time and bottle volume. Cont. Shelf Res. **31:** 496–506, doi:10.1016/j.csr.2010.07.006

Gillooly, J. F., J. H. Brown, G. B. West, V. M. Savage, and E. L. Charnov. 2001. Effects of size and temperature on metabolic rate. Science **293:** 2248–2251, doi:10.1126/science.1061967

Gist, N., P. Serret, E. M. S. Woodward, K. Chamberlain, and C. Robinson. 2009. Seasonal and spatial variability in plankton production and respiration in the Subtropical Gyres of the Atlantic Ocean. Deep Sea Res. II **56:** 931–940, doi:10.1016/j.dsr2.2008.10.035

Gosselin, M. 1997. New measurements of phytoplankton and ice algal production in the Arctic Ocean. Deep Sea Res. II **44:** 1623–1644, doi:10.1016/S0967-0645(97)00054-4

Gruber, N., and others. 2009. Oceanic sources, sinks, and transport of atmospheric CO_2. Global Biogeochem. Cycles **23:** GB1005, doi:10.1029/2008GB003349

Hein, M., and K. Sand-Jensen. 1997. CO_2 increases oceanic primary production. Nature **388:** 526–527, doi:10.1038/41457

Hood, E., J. Fellman, R. G. M. Spencer, P. J. Hernes, R. Edwards, D. D'Amore, and D. Scott. 2009. Glaciers as a source of ancient and labile organic matter to the marine environment. Nature **462:** 1044-U1100, doi:10.1038/nature08580

Jensen, L. M. [ed.], Nuuk ecological research operations, 5th Annual Report, 2011. Aarhus University, DCE–Danish Centre for Environment and Energy.

Kirchman, D. L., X. A. G. Moran, and H. Ducklow. 2009. Microbial growth in the polar oceans—role of temperature and potential impact of climate change. Nat. Rev. Microbiol. **7:** 451–459.

Kirk, J. 1994. Light and photosynthesis in aquatic ecosystems, 2nd ed. Cambridge Univ. Press.

Krause-Jensen, D., and others. 2012. Seasonal sea ice cover as principal driver of spatial and temporal variation in depth extension and annual production of kelp in Greenland. Global Change Biol. **18:** 2981–2994, doi:10.1111/j.1365-2486.2012.02765.x

Kritzberg, E. S., C. M. Duarte, and P. Wassmann. 2010. Changes in Arctic marine bacterial carbon metabolism in response to increasing temperature. Polar Biol. **33:** 1673–1682, doi:10.1007/s00300-010-0799-7

Labasque, T., C. Chaumery, A. Aminot, and G. Kergoat. 2004. Spectrophotometric Winkler determination of dissolved oxygen: Re-examination of critical factors and reliability. Mar. Chem. **88:** 53–60, doi:10.1016/j.marchem.2004.03.004

Laws, E. A. 1991. Photosynthetic quotients, new production and net community production in the open ocean. Deep Sea Res. **38:** 143–167, doi:10.1016/0198-0149(91)90059-O

Legendre, L. 1983. The ^{14}C method: Patterns of dark CO_2 fixation and DCMU correction to replace the dark bottle. Limnol. Oceanogr. **28:** 996–1003, doi:10.4319/lo.1983.28.5.0996

Lopez-Urrutia, A., E. San Martin, R. P. Harris, and X. Irigoien. 2006. Scaling the metabolic balance of the oceans. Proc. Natl. Acad. Sci. USA **103:** 8739–8744, doi:10.1073/pnas.0601137103

McClelland, J. W., R. M. Holmes, K. H. Dunton, and R. W. Macdonald. 2012. The Arctic Ocean estuary. Estuaries Coasts **35:** 353–368, doi:10.1007/s12237-010-9357-3

Middelboe, M., R. N. Glud, and M. K. Sejr. 2012. Bacterioplankton—key players in subarctic carbon cycling: A seasonal study on microbial activity and virus-induced mortality in Kobbefjord, Greenland. Limnol. Oceanogr. **57:** 1732–1742, doi:10.4319/lo.2012.57.6.1732

———, and C. Lundsgaard. 2003. Microbial activity in the Greenland Sea: Role of DOC lability, mineral nutrients and temperature. Aquat. Microb. Ecol. **32:** 151–163, doi:10.3354/ame032151

Moran, X. A. G., J. M. Gasol, C. Pedros-Alio, and M. Estrada. 2001. Dissolved and particulate primary production and bacterial production in offshore Antarctic waters during austral summer: Coupled or uncoupled? Mar. Ecol. Prog. Ser. **222:** 25–39, doi:10.3354/meps222025

Mortensen, J., K. Lennert, J. Bendtsen, and S. Rysgaard. 2011. Heat sources for glacial melt in a sub-Arctic fjord (Godthabsfjord) in contact with the Greenland Ice Sheet. J. Geophys. Res. Oceans **116:** C01013, doi:10.1029/2010JC006528

Nakaoka, S.-I., S. Aoki, T. Nakazawa, G. Hashida, S. Morimoto, T. Yamanouchi, and H. Yoshikawa-Inoue. 2006. Temporal and spatial variations of oceanic pCO_2 and air–sea CO_2 flux in the Greenland Sea and the Barents Sea. Tellus **58:** 148–161, doi:10.1111/j.1600-0889.2006.00178.x

Nguyen, D., R. Maranger, J. E. Tremblay, and M. Gosselin. 2012. Respiration and bacterial carbon dynamics in the Amundsen Gulf, western Canadian Arctic. J. Geophys. Res. Oceans **117:** C00G16, doi:10.1029/2011JC007343

Pomeroy, L. R., and W. J. Wiebe. 1993. Seasonal uncoupling of the microbial loop and its potential significance for the global cycle of carbon. Span. Soc. Microbiol.

Press, W., B. Flannery, S. Teukolsky, and W. Vetterling. 1986. Numerical recipes: the art of scientific computing. Cambridge University Press.

Rabe, B., and others. 2011. An assessment of Arctic Ocean freshwater content changes from the 1990s to the 2006–2008 period. Deep Sea Res. I **58:** 173–185, doi:10.1016/j.dsr.2010.12.002

Regaudie-De-Gioux, A., and C. M. Duarte. 2010. Plankton metabolism in the Greenland Sea during the polar summer of 2007. Polar Biol. **33:** 1651–1660, doi:10.1007/s00300-010-0792-1

———, and ———. 2012. Temperature dependence of planktonic metabolism in the ocean. Global Biogeochem. Cycles **26:** GB1015, doi:10.1029/2010gb003907

Richter, A., S. Rysgaard, R. Dietrich, J. Mortensen, and D. Petersen. 2011. Coastal tides in West Greenland derived from tide gauge records. Ocean Dyn. **61:** 39–49, doi:10.1007/s10236-010-0341-z

Riebesell, U., and others. 2007. Enhanced biological carbon consumption in a high CO_2 ocean. Nature **450:** 545–548, doi:10.1038/nature06267

Ruiz-Halpern, S., M. K. Sejr, C. M. Duarte, D. Krause-Jensen, T. Dalsgaard, J. Dachs, and S. Rysgaard. 2010. Air–water exchange and vertical profiles of organic carbon in a subarctic fjord. Limnol. Oceanogr. **55:** 1733–1740, doi:10.4319/lo.2010.55.4.1733

Rysgaard, S., T. Nielsen, and B. Hansen. 1999. Seasonal variation in nutrients, pelagic primary production and grazing in a high-Arctic coastal marine ecosystem, Young Sound, Northeast Greenland. Mar. Ecol. Prog. Ser. **179:** 13–25, doi:10.3354/meps179013

———, and M. Sejr. 2007. Vertical flux of particulate organic matter in a High Arcic fjord: Relative importance of terrestrial and marine sources, p. 109–121. *In* S. Rysgaard and R. Glud [eds.], Carbon cycling in Arctic marine ecosystems: Case study Young Sound. Medd Groenland.

———, AND OTHERS. 2012. High air–sea CO_2 uptake rates in nearshore and shelf areas of Southern Greenland: Temporal and spatial variability. Mar. Chem. **128:** 26–33, doi:10.1016/j.marchem.2011.11.002

SAKSHAUG, E., G. JOHNSEN, AND K. KOVACS. 2009. Ecosystem Barents Sea. Tapir Academic Press.

SEJR, M. K., M. BLICHER, AND S. RYSGAARD. 2009. Spatial and temporal variation in sea ice cover influence annual growth of the Arctic cockle *Clinocardium ciliatum* in Greenland. Mar. Ecol. Prog. Ser. **389:** 149–158, doi:10.3354/meps08200

———, D. KRAUSE-JENSEN, S. RYSGAARD, L. L. SORENSEN, P. B. CHRISTENSEN, AND R. N. GLUD. 2011. Air–sea flux of CO_2 in arctic coastal waters influenced by glacial meltwater and sea ice. Tellus B **63:** 815–822, doi:10.1111/j.1600-0889.2011.00540.x

———, T. G. NIELSEN, S. RYSGAARD, N. RISGAARD-PETERSEN, M. STURLUSON, AND M. E. BLICHER. 2007. Fate of pelagic organic carbon and importance of pelagic–benthic coupling in a shallow cove in Disko Bay, West Greenland. Mar. Ecol. Prog. Ser. **341:** 75–88, doi:10.3354/meps341075

———, M. WIODARSKA-KOWALCZUK, J. LEGEZYŃSKA, AND M. BLICHER. 2010. Macrobenthic species composition and diversity in the Godthaabsfjord system, SW Greenland. Polar Biol. **33:** 421–431, doi:10.1007/s00300-009-0717-z

SERRET, P., E. FERNANDEZ, J. A. SOSTRES, AND R. ANADON. 1999. Seasonal compensation of microbial production and respiration in a temperate sea. Mar. Ecol.-Prog. Ser. **187:** 43–57, doi:10.3354/meps187043

STEEMANN NIELSEN, E. 1952. The use of radioactive carbon (CM) for measuring organic production in the sea. J. Cons. Cons. Int. Explor. Mer **18:** 117–140, doi:10.1093/icesjms/18.2.117

TAKAHASHI, T., AND OTHERS. 2002. Global sea–air CO2 flux based on climatological surface ocean $P_{CO}2$, and seasonal biological and temperature effects. Deep Sea Res. II **49:** 1601–1622, doi:10.1016/S0967-0645(02)00003-6

TANG, K. W. 2011. Metazooplankton community structure, feeding rate estimates, and hydrography in a meltwater-influenced Greenlandic fjord. Mar. Ecol. Prog. Ser. **434:** 77–90, doi:10.3354/meps09188

TREMBLAY, J.-É., K. G. SIMPSON, J. MARTIN, L. MILLER, Y. GRATTON, D. BARBER, AND N. M. PRICE. 2008. Vertical stability and the annual dynamics of nutrients and chlorophyll fluorescence in the coastal, southeast Beaufort Sea. J. Geophys. Res. **113:** C07S90, doi:10.1029/2007jc004547

WANNINKHOF, R. 1992. Relationship between wind speed and gas exchange over the ocean. J. Geophys. Res. **97:** 7373–7382, doi:10.1029/92JC00188

WEISS, R. 1974. Carbon dioxide in water and seawater: The solubility of a non-ideal gas Mar. Chem. **2:** 203–215.

Associate editor: George W. Kling

Received: 23 August 2013
Accepted: 29 April 2014
Amended: 26 June 2014